

Microphase Separation and Rheological Properties of Polyurethane Melts. 2. Effect of Block Incompatibility on the Microstructure

Sachin Velankar and Stuart L. Cooper*[†]

Department of Chemical Engineering, University of Delaware, Newark, Delaware 19716

Received May 25, 1999; Revised Manuscript Received October 29, 1999

ABSTRACT: This second paper in this series regarding the relationship between structure and viscoelastic properties of multiblock polyurethane elastomers presents the results of varying segmental incompatibility at fixed segment length and composition. Three series of amorphous polyurethanes with pendant trimethylammonium groups were synthesized. Quaternization of these groups with iodomethane caused segmental incompatibility to increase in a controlled fashion without significantly affecting the block length, composition, or molecular weight. This gave three series of polyurethanes with varying incompatibility; their microstructures have been characterized in this paper and their viscoelastic properties, in the accompanying paper. DSC experiments showed that increasing incompatibility caused microphase separation and that the polyurethanes ranged from almost homogeneous to highly microphase-separated. All polyurethanes showed a peak in their SAXS data. The peak intensity was independent of temperature for all materials studied except one, which showed a decrease in intensity with increasing temperature. This was found to be in accordance with a mean-field-like approach to a spinodal temperature that was well below room temperature, although this polyurethane showed strong microphase separation even at room temperature. In accordance with past research on polyurethanes, there was no evidence for long-range lamellar order in the microphase-separated structure for any polyurethane studied. This paper demonstrates that in such a situation rigorously distinguishing between the homogeneous and the microphase-separated states is a difficult task, and the concept of a binodal separating these two states is highly ambiguous.

1. Introduction

Polyurethanes^{1–3} (PUs) are an important class of thermoplastic elastomers with wide applications as coatings, binder resins, fibers, and high-performance elastomeric products. Typical PU elastomers are multiblock copolymers comprised of alternating “soft” polyether or polyester segments and “hard” polyurethane segments. Thermodynamic incompatibility of these segments, often combined with crystallization of either or both segments, drives their microphase separation into hard and soft domains that are respectively below and above their glass transition temperatures. This microphase separation is responsible for the excellent elastomeric properties of polyurethanes.

As pointed out in the first part of this series,⁴ there are three principal parameters that govern the properties of polyurethane elastomers: block length N , block incompatibility χ , and composition. That paper investigated the effect of block length on the “E-series” polyurethanes, keeping the other two parameters constant. This and the accompanying paper describe the effects of incompatibility keeping the segment length and composition constant. In addition, the present research is more rigorous in that the effects of incompatibility have been measured at fixed molecular weight, as described below.

It is well-known that the thermal and mechanical properties of polymers below their T_g (in the case of polyurethanes, the hard segment T_g) become independent of molecular weight at sufficiently high molecular weight. This obviously does not hold for viscoelastic properties of melts; terminal viscosity and relaxation time are known to increase monotonically with molec-

ular weight.⁵ The previous work⁴ ignored effects of MW and concentrated only on the effects of block molecular weight (or block length). Thus, it was implicitly assumed that the effects of block length dominated over those of MW, a reasonable assumption if the MW is large enough to render insignificant any “end effects” related to number of blocks per chain. If this assumption fails, it is most likely to do so in the terminal region where effects of MW are most severe, especially if the polymer is entangled. This assumption was tested at the end of that paper⁴ and found to be reasonably valid. In any case, two of the four samples of the E-series had molecular weights close to each other as did the other two, allowing them to be compared more or less rigorously. However, this was entirely fortuitous, and to be truly rigorous, some means of synthesizing polyurethanes with fixed molecular weight and variable incompatibility is desired for the present work.

Traditionally, the degree of polymerization obtained from condensation polymerization reactions is controlled by two means: employing stoichiometrically unbalanced reactants and controlling the conversion of the reaction by limiting the removal of a byproduct.⁶ Neither of these is suitable for polyurethanes, the first because the diisocyanate reactants have limited purity and the second because the urethane condensation reaction has no byproduct. Therefore, synthesizing polyurethanes of a desired molecular weight is not an easy exercise. For the present purposes of changing block incompatibility, it is far preferable to synthesize a single polyurethane and then to chemically alter either or both blocks *after* synthesis so as to change their relative incompatibility. At least one such possible scheme based on polyurethanes with polybutadiene soft segments has been detailed by Chen et al.⁷ In their approach, controlled epoxidation of the diene after polyurethane synthesis

[†] Present address: Illinois Institute of Technology, 10 W. 32nd St., Chicago, IL 60616.

causes an increase in the polarity of the soft segment, thereby making it more compatible with the hard segment. This paper utilizes another such technique of selectively altering one block of a polyurethane as described below.

Goddard and Cooper⁸ synthesized polyurethanes with hard segments that had pendant trialkylammonium groups and quaternized them with alkyl halides. The polyurethane cationomers thus formed were shown to have better microphase separation and hence far superior mechanical properties than their nonionic precursors; however, no evidence of ionic aggregation was found in the cationomers. Subsequent infrared spectroscopic experiments⁹ showed that the improvement of microphase separation was due to strong hydrogen bonding between the iodide and the urethane N-H groups, rather than due to ionic aggregation. Similar lack of ionic aggregation and hydrogen bonding of the anions has been demonstrated in other cationomers (see references in Goddard and Cooper⁹). It is well-known that inter-urethane hydrogen bonding between the carbonyl and N-H groups is one of the major driving forces for microphase separation in polyurethanes. The fact that it is stronger hydrogen bonding rather than ionic aggregation that improves the microphase separation in quaternary ammonium polyurethanes implies that they are similar to traditional polyurethanes rather than to ionomers. From an experimental viewpoint, such polyurethane cationomers have an advantage over nonionic polyurethanes in that the segmental incompatibility can be controlled very easily through the extent of quaternization. Specifically, an increase in the extent of quaternization corresponds to a greater incompatibility (due to stronger interurethane hydrogen bonding), with negligible change in overall molecular weight. Hence, such polyurethane cationomers may be used in the present study as model systems for polyurethanes with variable segmental incompatibility.

The MDI/BD-based PUs (i.e., hard segments composed of 4,4'-diphenylmethane diisocyanate and 1,4-butanediol) studied by Goddard and Cooper are unsuitable for rheological studies due to the low degradation temperature of aromatic isocyanates and the high T_g of the hard segments. Goddard and Cooper did attempt to study high-temperature microphase mixing in their materials by rheological and other techniques,¹⁰ but detailed rheological characterization was not possible. The requirements for a polyurethane to be suitable for rheological studies have been detailed previously.⁴ Following those criteria, isophorone diisocyanate (IPDI) was chosen as the diisocyanate, rather than MDI. The chain extender employed here, dimethylamino-1,2-propanediol (DMP), is identical to that used by Goddard and Cooper.⁸⁻¹⁰ Poly(propylene oxide) (PPO) has been chosen as the soft segment rather than the previous choice of polycaprolactone in order to avoid crystallinity and therefore allow experiments below 50 °C. The structure of these materials is shown in Scheme 1, and other details are given in Table 1. The hydrogen bonding between the iodide and the urethane N-H was verified by infrared spectroscopy.¹¹ Structural investigations of these materials by calorimetry and SAXS are described here, and the companion paper discusses corresponding linear viscoelastic properties.

2. Experimental Section

2.1. Synthesis and Chemical Characterization. Hydroxy-terminated PPO of various molecular weights and DMP

Scheme 1. Structures of Polyurethane Cationomers

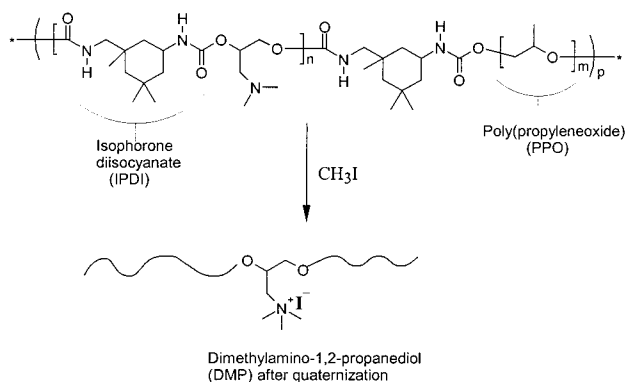


Table 1. Structural Characteristics of Polyurethane Cationomers

sample	soft-segment mol wt	wt-av MW	wt % soft segment ^a	% quaternization ^b
I725-0			48	0
I725-12	725	40000	47	12
I725-25			46	25
I725-40			45	40
I1000-0			47	0
I1000-13	1000	36000	46	13
I1000-32			45	32
I1000-40			45	40
I2000-0			57	0
I2000-14	2000	29000	55	14
I2000-29			54	29
IPDI/DMP		36700	0	

^a Estimated error $\pm 2\%$. ^b Estimated error $\pm 3\%$.

were dried in a vacuum for several hours before use. IPDI and dibutyltin dilaurate were used as received. Two-step solution polymerizations were conducted following standard methods¹² using *N,N*-dimethylacetamide (DMAc) as solvent and dibutyltin dilaurate as catalyst. All chemicals were purchased from Aldrich Chemical Co. Reactions followed the procedure described earlier,⁴ and the temperature was kept low (<55 °C) during these reactions to prevent any branching side reactions. The polymers were precipitated in distilled water and dried in a vacuum at 0.1 Torr and 50 °C for at least 2 days. This was followed by Soxhlet extraction with heptane and redrying in a vacuum. Quaternization was achieved by dissolving the polyurethanes in DMAc to approximately 15 wt % and adding the appropriate amount of iodomethane dissolved in DMAc for the desired extent of quaternization. The solutions turned yellow in a few minutes, and the reactions were allowed to continue at room temperature for an hour and then for 5–6 h at 50 °C. The solutions were filtered and cast onto Teflon plates. Cast solutions were dried at 40–45 °C in air for 3–4 days, and then the films were dried at 35–40 °C in a vacuum for a further 3–4 days to obtain films of about 0.4 mm thickness which were stored in desiccators.

Molecular weights were measured prior to quaternization by gel permeation chromatography (GPC) as described previously.⁴ As in the previous study, all materials described here had approximately 50 wt % of soft segments and polydispersity indices between 1.5 and 1.8. GPC traces of unquaternized samples recovered from extended rheological testing, as well as those of samples held at 140 °C for 2 h in air, were identical to those of the starting polyurethanes, thereby eliminating the possibility of mechanical relaxation due to bond breakage. Using quantitative ¹³C NMR experiments (see below) before and after annealing at high temperature, it was found that dequaternization reactions were insignificant below 120 °C. At 140 °C, significant dequaternization occurred over time scales of SAXS experiments, and hence the SAXS experiments were not performed above 120 °C.

Compositions of the materials were found using quantitative ¹³C nuclear magnetic resonance (NMR) spectroscopy on a 240

MHz instrument (Bruker). The polyurethanes were dissolved in deuterated dimethyl sulfoxide, and the NMR experiments were carried out at 60 °C with a data acquisition delay of 30 s. The extents of quaternization were also determined from the same data by comparing the areas corresponding to the NMR peaks of methyl groups of the chain extender ($\delta = 46$ ppm and $\delta = 53.3$ ppm for methyl groups attached to tertiary and quaternary nitrogens, respectively). Molecular weights, compositions, and extents of quaternization of the materials used in this study are presented in Table 1. Materials are designated as I_{x-y} where x is the molecular weight of the soft segment and y the percentage of DMP that has been quaternized. The three series of materials differ primarily in the molecular weight of the segments, and materials within each series differ primarily in the amount of quaternization, i.e., in the segmental incompatibility. All materials have about 50% soft segment, implying that the average molecular weights of the soft and the hard blocks are roughly equal.

2.2. DSC Experiments. DSC experiments were performed as described previously.⁴ It was found that rheometric measurements on as-cast samples were not reproducible; hence, samples were annealed at 55 °C for 12–14 h prior to rheological experiments.¹³ For consistency, the same thermal history was imposed upon all samples prior to DSC experiments as well. Samples were transferred from the oven to the DSC, annealed at 55 °C for a further 2 min, and quenched to -130 °C at 320 °C/min (nominal rate). The sample was held at -130 °C for about 3–4 min until the heat flow stabilized and then scanned at 20 °C/min.

2.3. SAXS Experiments. SAXS experiments and data processing were performed as described previously.⁴ For the reasons mentioned in the previous section, all samples were annealed at 55 °C in an oven prior to SAXS experiments. Each sample was first measured at 30 °C and then at successively higher temperatures in 10 °C increments. Sample transmittance was measured before and after each measurement; a change in transmittance was regarded as evidence of sample flow, and measurements at higher temperatures were continued with a fresh sample. A few samples were remeasured at 30 °C after high-temperature experiments, and their scattering was found to be almost identical to that before the high-temperature experiments.

3. Results

3.1. DSC Data. 3.1.1. Effect of Quaternization on the Thermal Properties of the Pure Hard Segment. The thermal properties of the polyurethanes, the pure PPO precursors, and the hard segment IPDI/DMP quaternized to various extents can be measured directly by DSC. Since neither the soft nor the hard segment is crystallizable, the only complication to be considered is the effect of the amount of quaternization on the T_g and ΔC_p of the hard segment. Figure 1a shows the effect of quaternization on the T_g of IPDI/DMP quaternized to various extents. The top curve shows a large overshoot in the first scan of as-cast samples quenched from room temperature. This overshoot is seen for the first heats of all other samples (not shown) and is not highly reproducible. Reproducible data were obtained upon cooling the samples after 2 min at 140 °C and repeating the scan. These glass transition temperatures are plotted in Figure 1b against the extents of quaternization, along with an empirical quadratic fit. This quadratic fit is then used to calculate the T_g 's of the hard segments of the polyurethane cationomers from their extents of quaternization as measured by ¹³C NMR; these are presented in the fourth column of Table 2. The ΔC_p at the glass transition is found to be 0.38 ± 0.05 J/(g K) for all the quaternized hard segments.

3.1.2. Qualitative Assessment. As mentioned in section 2.2, only samples annealed at 55 °C are relevant

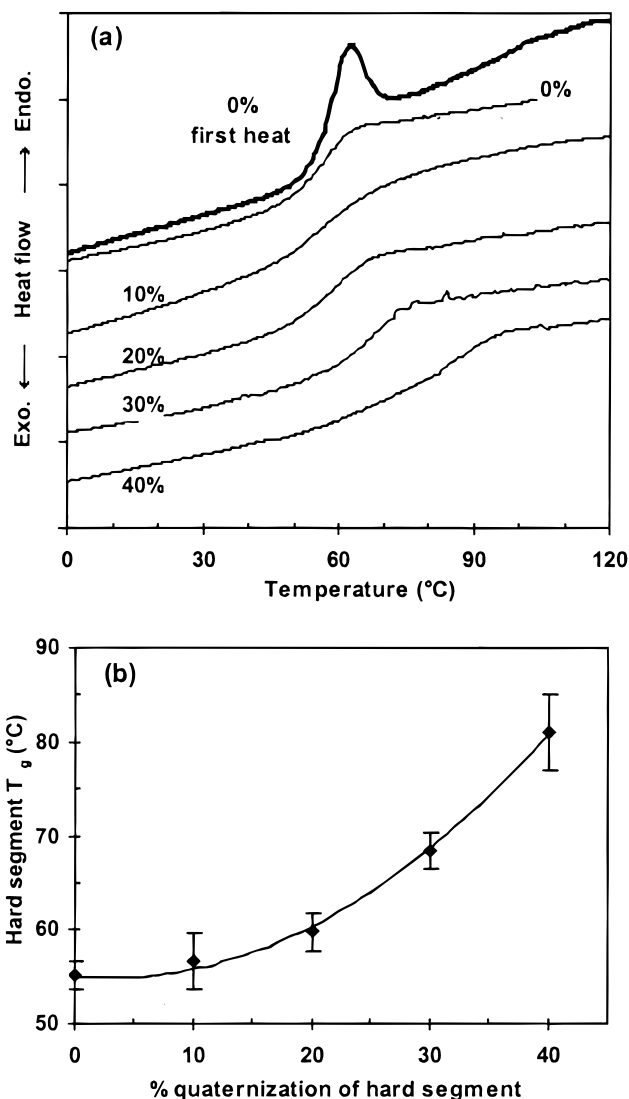


Figure 1. Effect of the extent of quaternization on the hard-segment T_g . (a) DSC traces of pure hard segments with various degrees of quaternization: top curve is first heat; all others are cooled from 140 °C. Each tic on the y -axis is 0.2 J/(g K). (b) T_g 's measured from second heat traces in (a) and a quadratic fit.

to the analysis of the rheological properties. However, the DSC traces of as-cast samples showed interesting endotherms, and hence these are presented below as well.

Figure 2 shows that DSC traces of all polyurethanes based on the PPO-725 precursor are almost featureless, except for a broad glass transition at a temperature intermediate to that of the pure hard and pure soft segments. Annealing at higher temperatures (55 and 140 °C were tried with annealing times up to 30 min) followed by quenching to -130 °C and rescanning produced no changes in the DSC traces.

Figure 3 shows that the first heats of all polyurethanes based on PPO-1000 have two poorly resolved glass transitions, followed by a distinct endotherm at about 60 °C. The temperature and intensity of the endotherm are not highly reproducible; it is suspected that small differences in thermal history are responsible for this irreproducibility. Multiple melting endotherms are a characteristic feature of polyurethanes,^{14–17} and endotherms similar to those in Figure 3 have been

Table 2. Thermal Properties of Polyurethane Cationomers

sample	pure homopolymer properties				polyurethane properties			calculated properties			
	$T_{g,ss}$, °C	$\Delta C_{p,ss}$, J/(g K)	$T_{g,hs}$, °C	$\Delta C_{p,hs}$, J/(g K)	$T_{g,mi}$, °C	ΔC_p , J/(g K)	W_{ss}^a	ΔC_p^b , J/(g K)	T_g^c , °C	f_{ss}^d	F_{ss}^e
I725-0			55 ± 2	0.42 ± 0.05	3.6	0.42	0.48	0.56	-22.3	0.29	0.31
I725-12	-71.4 ± 1	0.72 ± 0.03	56	0.38	3.2	0.38	0.47	0.54	-23.6	0.27	0.29
I725-25			66	0.38	6.1	0.42	0.46	0.53	-18.7	0.29	0.32
I725-40			78	0.38	3.9	0.45	0.45	0.53	-12.6	0.34	0.35
I1000-0			55 ± 2	0.42 ± 0.05	<i>f</i>	<i>f</i>	0.47	0.55	-19.5		
I1000-13	-70.7 ± 1	0.69 ± 0.03	58	0.38	<i>f</i>	<i>f</i>	0.45	0.52	-19.1		
I1000-32			70	0.38	-33.1	0.124	0.44	0.52	-12.8	0.60	0.10
I1000-40			80	0.38	-34.5	0.129	0.43	0.51	-7.3	0.63	0.11
I2000-0			55 ± 2	0.42 ± 0.05	-52.1	0.254	0.57	0.56	-28.9	0.80	0.22
I2000-14	-69.2 ± 1	0.66 ± 0.03	57	0.38	-55	0.242	0.55	0.53	-28.7	0.82	0.22
I2000-29			66	0.38	-55	0.251	0.55	0.53	-26.0	0.83	0.23

^a Measured by quantitative ¹³C NMR; expected error ~3%. ^b From Couchman's eq 2, assuming no microphase separation. ^c From Couchman's eq 1. ^d From eq 3. ^e From eq 4. ^f Too indistinct to be reliably measured.

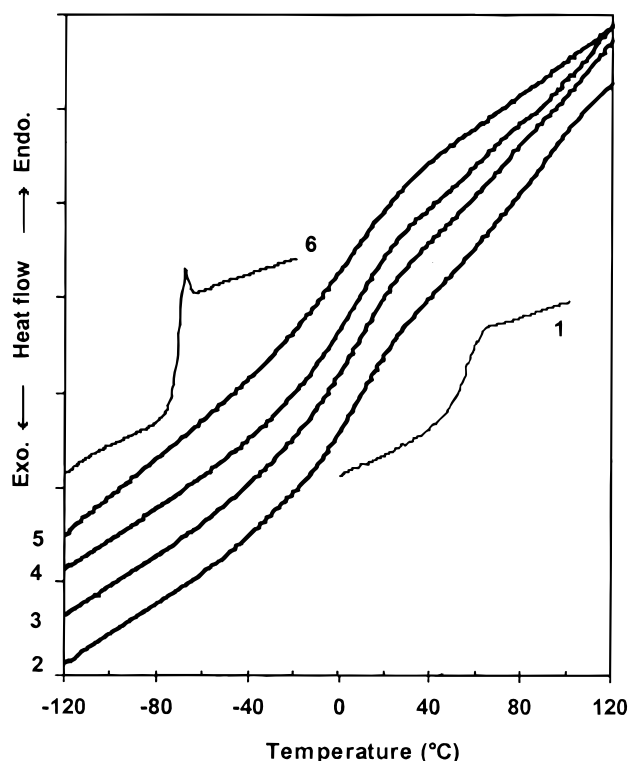


Figure 2. DSC traces of I725 series. Curves correspond to (1) pure IPDI/DMP, (2) I725-0, (3) I725-12, (4) I725-25, (5) I725-40, and (6) pure soft-segment PPO-830. Each tic on the y-axis is 0.2 J/(g K). All data shown are first heats. Annealing at 55 or 140 °C produces identical traces. Note that trace 1 refers to the hard segment of the unquaternized PU only. All other PUs have higher hard-segment T_g 's as per Figure 1.

observed before. They usually occur about 20 °C above the annealing temperature of the polyurethane; this is in accordance with the present temperature of 35–40 °C during film-drying. The mechanisms responsible for these endotherms are not well-understood, but they are highly sensitive to thermal history and are rarely visible on “second heat” DSC scans. These endotherms are not very important for the present work since they were completely erased upon annealing at 55 °C for 12 h (necessary for obtaining reproducible rheometric data as mentioned above). Finally, quenching from higher annealing temperatures (140 °C for 30 min) caused no change in the DSC traces of the I-1000 series of polyurethanes.

Similar, though somewhat more intense, endotherms are found in the DSC traces of the PPO-2000-based

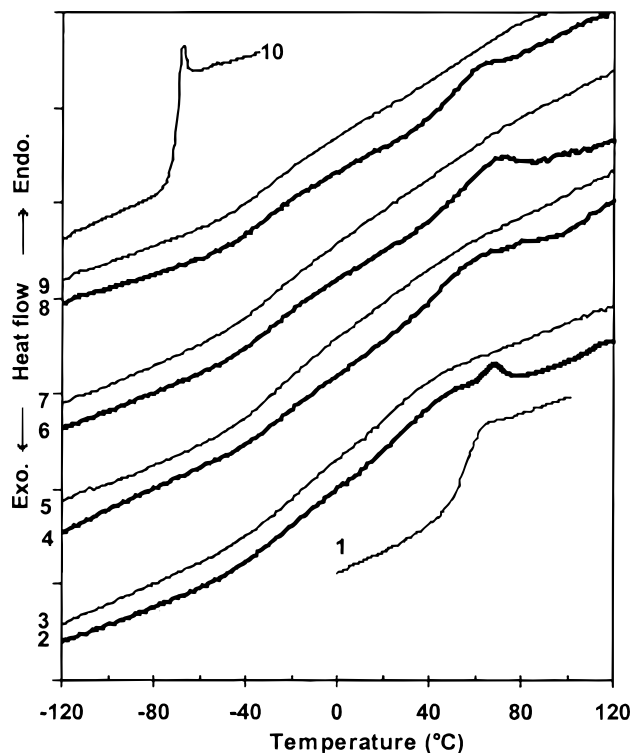


Figure 3. DSC traces of I1000 series. Curves correspond to (1) pure IPDI/DMP, (2, 3) I1000-0, (4, 5) I1000-13, (6, 7) I1000-33, (8, 9) I1000-40, and (10) pure soft-segment PPO-1000. Each tic on the y-axis is 0.2 J/(g K). Thick curves 2, 4, 6, and 8 are first heats; thin curves 3, 5, 7, and 9 are quenched from 140 °C. Annealing at 55 °C produces traces identical to those at 140 °C. Note that trace 1 refers to the hard segment of the unquaternized PU only. All other PUs have higher hard-segment T_g 's as per Figure 1.

polyurethanes of Figure 4 as well. These are also erased by annealing at 55 °C overnight, and once again, annealing at 140 °C does not affect the DSC curves. In all the I2000 materials, the soft segment glass transition is very sharply defined and occurs at a temperature relatively close to that of the pure soft segment, indicative of excellent microphase separation in this series.

Similar to the poly(ester urethane)s studied previously,⁴ the present polyurethane cationomers showed no change in their DSC traces when quenched from high temperatures. Hence once again, these DSC data do not allow us to draw microphase composition vs temperature phase diagrams.

3.1.3. Quantitative Analysis. Only the samples with the same thermal history as samples used in rheological

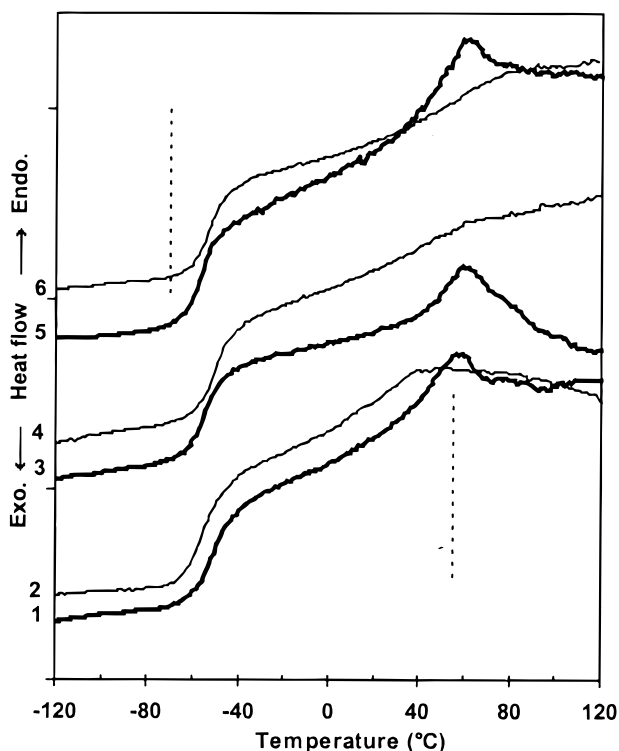


Figure 4. DSC traces of I2000 series. Curves correspond to (1, 2) I2000-0, (3, 4) I2000-14, and (5, 6) I2000-29. Each tic on the y -axis is 0.2 J/(g K). Thick curves 1, 3, and 5 are first heats; thin curves 2, 4, and 6 are quenched from 55 °C. Longer annealing at 55 °C or at higher temperatures causes no further change in the traces. Broken lines show T_g 's of the soft-segment homopolymer PPO-2000 and the hard-segment IPDI/DMP; the full curves have been omitted to allow an expanded scale.

experiments (i.e., 55 °C 12–14 h) are analyzed here. The characteristics of their soft-segment glass transition are listed in Table 2. In the first paper in this series,⁴ the following equations were used for quantitative thermal analysis.

$$T_g = \frac{w_{ss}T_{g,ss} + \alpha w_{hs}T_{g,hs}}{w_{ss} + \alpha w_{hs}} \quad (1)$$

$$\Delta C_p = w_{ss}\Delta C_{p,ss} + w_{hs}\Delta C_{p,hs} \quad (2)$$

$$f_{ss} = \frac{\alpha(T_{g,hs} - T_g)}{(T_g - T_{g,ss}) + \alpha(T_{g,hs} - T_g)} \quad (3)$$

$$F_{ss} = \frac{\Delta C_p}{f_{ss}\Delta C_{p,ss} + (1 - f_{ss})\Delta C_{p,hs}} \quad (4)$$

Here $T_{g,ss}$, $\Delta C_{p,ss}$, $T_{g,hs}$, and $\Delta C_{p,hs}$ are the glass transition temperature and change in heat capacity at the glass transition of the pure soft and hard segments, respectively, T_g and ΔC_p are the corresponding properties for the soft-segment-rich phase of the polyurethane, and $\alpha = \Delta C_{p,hs}/\Delta C_{p,ss}$. f_{ss} is the weight fraction of the soft segment in the soft-segment-rich phase, and F_{ss} is the weight fraction of the soft-segment-rich phase. w_{ss} and w_{hs} ($=1 - w_{ss}$) are the overall weight fractions of the soft and hard segments in the polyurethane and are close to 50% for all the materials studied here (Table 1). The first two equations are called Couchman's equations,¹⁸ and the third equation is an inversion of

the first, as applied to the soft-segment-rich phase. Note that eq 3 corrects a typographic error in the corresponding equation presented previously.⁴ The measured properties and the results of these calculations are presented in Table 2.

The measured polyurethane properties behave in an expected fashion: the unquaternized materials show a decrease in T_g as block length increases indicative of better microphase separation. Within each series, the T_g does not change significantly with increasing quaternization, except in the I1000 series where the T_g becomes better defined as per Figure 3. This is somewhat surprising since more quaternization is expected to improve microphase separation and hence lower the T_g . However, there is a competing effect: as quaternization increases, the T_g of the pure hard segment increases as well (Figure 1). Since some hard segment is usually dissolved in the soft-segment-rich phase (i.e., $f_{ss} < 1$), it causes the T_g of the soft segment phase to increase. Evidently, this is enough to offset the lowering of T_g due to better microphase separation. This discussion also implies that if the I725 materials were to be single-phase, their T_g should increase with quaternization. This is not seen in Table 2, indicating that the I725 materials are not completely homogeneous. Further analysis of the DSC traces shows slight broadening of the transition with quaternization (not clearly visible in Figure 2) which supports this view.

The ΔC_p values for the I725 polymers calculated assuming a weighted average (eq 2) are reasonably comparable to the measured ΔC_p , indicating that the I725 series is almost homogeneous, although there must be at least some microphase separation as per the last paragraph. However, Couchman's prediction (eq 1) for the T_g of this single phase is in gross disagreement with the measured T_g ; moreover, since the prediction is far lower than the T_g , the discrepancy cannot be attributed to slight microphase separation. Nor is this an artifact of using Couchman's equations; the results from the more commonly used Fox equation are almost the same. The microphase compositions predicted by eq 3 are also unphysical since $f_{ss} > w_{ss}$ must hold by definition. This puts the validity of applying eqs 1–4 to these materials in doubt; nevertheless, the rest of the calculations in Table 2 are more reasonable. They indicate that the soft-segment-rich phase in the I2000 series is fairly pure ($f_{ss} \sim 0.8$) although the weight fraction of this phase is relatively small (~ 0.2). Since a well-defined hard segment T_g is not visible, the fraction of the hard-segment-rich phase F_{hs} must also be small. The overall composition is close to 50% soft segment, and hence a large fraction of this material must reside in the interface between the lamellae and undergo a glass transition at temperatures between the T_g and $T_{g,hs}$. We reemphasize that the quantitative aspects of these calculations are not likely to be very accurate.

Thus, to briefly summarize, DSC data indicate that microphase separation increases with segment length, with the I725 series being more or less homogeneous and the I2000 series being considerably microphase-separated. There is no appreciable change in the T_g upon changing the extent of quaternization (i.e., block incompatibility).

3.2. Small-Angle X-ray Scattering. 3.2.1. SAXS Theory, Background Subtraction, and Normalization of Intensities. The X-ray scattering from heterogeneous materials is given by^{19,20}

$$\frac{I(q)}{VI_e(q)} = 4\pi\Delta\rho^2 \int_0^\infty r^2 \gamma(r) \frac{\sin(qr)}{qr} dr \quad (5)$$

where the left-hand side is the scattering intensity normalized by the single electron scattering $I_e(q)$ and the sample volume V , and $\Delta\rho^2$ is the mean-square amplitude of the electron density fluctuations. The correlation function $\gamma(r)$, which is given by

$$\gamma(r) = \frac{1}{Q} \int_0^\infty q^2 \frac{I(q)}{VI_e(q)} \frac{\sin(qr)}{qr} dq \quad (6)$$

contains all the information about the spatial extent of the heterogeneity in the material and none about its amplitude. The invariant Q is the integral of the Lorentz-corrected (i.e., q^2 weighted) intensity

$$Q = \int_0^\infty q^2 \frac{I(q)}{VI_e(q)} dq = 2\pi^2 \overline{\Delta\rho^2} \quad (7)$$

For the present purposes, we will regard the polyurethanes as being two-phase materials. For an ideal two-phase material (i.e., constant density within each phase, sharp interfaces),

$$Q_{\max} = 2\pi^2 \phi_1 \phi_2 (\rho_1 - \rho_2)^2 \quad (8)$$

where ρ_1 and ρ_2 are the electron densities and ϕ_1 and ϕ_2 are the volume fractions of the two phases. If the ratio Q/Q_{\max} is close to 1, it is indicative of good microphase separation whereas a value much lower than 1 may result from microphase mixing either at the interface or in the bulk. In the polyurethane literature Q/Q_{\max} has been used as a definition of the degree of microphase separation and is often found to be quite low (between 0.2 and 0.5).^{17,21–23} However, numerical values of Q/Q_{\max} should be used with caution.²⁴

Equations 5–7 describe scattering from heterogeneities in electron density; in addition, the measured SAXS intensity includes contributions from other sources such as thermal density fluctuations, the amorphous halo of the WAXS extending to small angles, etc.^{19,20} The sum of all these contributions is called the SAXS background. This is either constant or increasing with q and must be subtracted from the measured intensity before information about the heterogeneity may be obtained from the data. A common form used for the SAXS background is²⁰

$$I_b(q) = a + bq^m \quad (9)$$

where m may be taken to be 4;²⁵ the second term representing the amorphous portion of the WAXS may be omitted if the intensity does not show an upturn at high q . If data are available up to sufficiently high q where I_b dominates over scattering from the heterogeneous structure, the parameters a , b , and m may be reliably estimated. Some of the present samples showed a peak at fairly high q , and therefore the q range of the experimental apparatus was not sufficient to allow measurement of intensity in a region of dominant I_b . In other samples with a peak at relatively low q , the q range was sufficient to see an upturn at high q , allowing a , b , and m to be obtained. In two such samples, however, m was found to be unreasonably low (<1).

Table 3. Scattering Characteristics of Polyurethane Cationomers

sample	n	k^a nm ³	m^b nm ⁻¹	w^c nm ⁻¹	q_{\max}^d nm ⁻¹	$k(m^2 + w^2)^e$ nm
I725-12	1.35 ± 0.5	0.17	1.59	1.31	2.67	0.72
I725-25	3.74 ± 0.4	0.13	1.41	0.79	1.85	0.34
I725-40	3.99 ± 0.3	0.24	1.41	0.65	1.72	0.59
I1000-0	4.36 ± 0.4	0.068	1.43	0.62	1.70	0.17
I1000-13	3.10 ± 0.5	0.23	1.12	0.71	1.57	0.40
I1000-32	3.52 ± 0.4	0.40	1.08	0.53	1.34	0.58
I1000-40	3.98 ± 0.2	0.54	1.07	0.46	1.28	0.74
I2000-0	4.65 ± 0.4	0.7	1.00	0.38	1.14	0.80
I2000-14	4.28 ± 0.2	0.96	0.95	0.31	1.05	0.96
I2000-29	4.44 ± 0.2	1.50	0.94	0.25	1.01	1.42

^a Variation in peak intensity is 15% for I725-12 and about 5% for other samples. ^b Error bars are about ±0.05 nm⁻¹ for I725 series and I1000-0 and about ±0.02 nm⁻¹ for the remaining samples. ^c Error bars are ±0.15 nm⁻¹ for I725-12 and about ±0.07 nm⁻¹ for the other samples. ^d Lorentz-corrected peak position: $q_{\max} = m + w^2/m$. ^e Lorentz-corrected peak intensity.

Thus, to maintain consistency across all samples, a constant background was assumed for all samples.

For some samples, the value of the constant I_b had to be estimated from regions of the data where I_b was not dominant; therefore, contributions from eq 5 had to be accounted for when estimating I_b . At high q , scattering from an ideal two-phase sample (i.e., sharp phase boundaries) is expected to follow Porod's law: $I(q) \sim q^{-4}$. In our previous work, all samples were found to obey q^{-4} at high q despite the fact that sharp phase boundaries were not expected, allowing I_b to be estimated by fitting high- q data to $a + cq^{-4}$. In the present samples, agreement with Porod's law was reasonable (except for I725-12) but not excellent. Data could be fit much better by allowing the scattered intensity to follow $I(q) \sim q^{-n}$ at high q . Hence, this form was used to fit the data; the corresponding values of n have been listed in Table 3. It should be noted that some samples have $n < 4$; i.e., $I(q)$ decreases slower than q^{-4} . Such behavior cannot be captured by using Porod's law modified for diffuse interfaces^{23,26,27} for which $I(q)$ decreases faster than q^{-4} .

Thus, to summarize the background subtraction procedure, the measured $I(q)$ data were fit to

$$I(q) = a + cq^{-n} \quad (10)$$

using the "gnufit" software, and the data between $q = 1.5q_{\max}$ and $3q_{\max}$ were used for these fits. For some samples (especially the I2000 series) data extended to sufficiently high q where I_b was dominant. For these samples, the values of a from eq 10 were found to be almost equal those estimated by fitting eq 9 to the I_b dominant regions lending confidence to the background subtraction procedure. All analysis was based on data after subtracting $I_b = a$; the only remaining correction to the data is the normalization described next.

It is desired to evaluate the effect of segmental incompatibility on the SAXS patterns and therefore on microphase separation. In this work, segmental incompatibility has been increased by increasing the quaternization of the hard segment. This causes an increase in the electron density of the hard segment and hence in the electron density contrast between the soft and hard segments. As per eqs 5, 7, and 8, scattering intensity is proportional to the square of the electron density contrast. Thus, I2000-29 would show a higher scattering intensity than I2000-0 even if they had exactly identical microstructures (i.e., identical $\gamma(r)$).

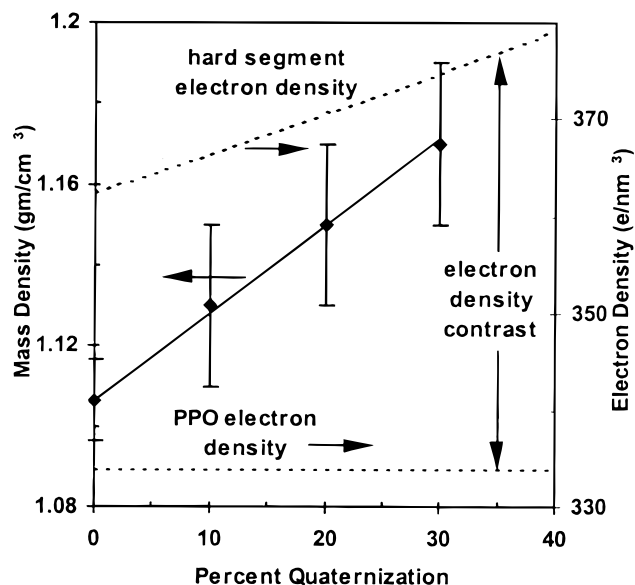


Figure 5. Effect of the extent of quaternization on the mass and electron density of the hard segments of polyurethane cationomers. Solid diamonds and solid line refer to the left axis whereas the broken lines refer to the right-hand axis.

because I2000-29 has a higher electron density contrast than I2000-0. Therefore, before comparing SAXS patterns to evaluate the effects of segmental incompatibility, the intensities must be normalized by $Q_{\max} = 2\pi^2\phi_{SS}\phi_{HS}(\rho_{HS} - \rho_{SS})^2$. These electron densities of the hard and soft segments may be obtained by

$$\rho_{\text{segment}} = \frac{(\text{electrons/repeat unit})(\text{density of segment})N_{\text{Av}}}{\text{molecular weight of repeat unit}} \quad (11)$$

The mass density of poly(propylene oxide), obtained from the information provided by the supplier (Aldrich Chemical Co.), is 1.005 g/cm³, giving an electron density $\rho_{SS} = 334 \text{ e}^-/\text{nm}^3$. The mass density of the hard segment may be expected to vary with the extent of quaternization; mass densities of the pure IPDI/DMP and of three more quaternization levels were measured by immersion in aqueous NaCl solutions of known concentration. These are presented in Figure 5, along with a linear fit. IPDI/DMP with 40% quaternization was found to be too brittle to handle, and hence, its mass density was estimated by extrapolation of the straight line. The broken line in Figure 5 shows the dependence of electron density of the hard segment ρ_{HS} on the extent of quaternization (eq 11). The calculated Q_{\max} may be used to normalize the data. Note that $\phi_{SS}\phi_{HS}$ is almost equal for all materials since all have about 50 wt % of the hard and soft segment; thus, the primary normalization required is $(\rho_{HS} - \rho_{SS})^2$.

3.2.2. Qualitative Analysis of Scattering Data.

Figure 6 shows the effect of quaternization on the normalized SAXS patterns of the I725 series. I725-0 (not shown) showed a very weak peak in the scattering data between about $q = 2$ and 2.5 nm^{-1} , but effective background subtraction could not be performed. Similar results for the I1000 and I2000 series are shown in Figures 7 and 8, respectively. In every case, quaternization causes an increase in the scattering intensity, a decrease in peak width, and a decrease in the peak position; the last corresponds to increase in the long

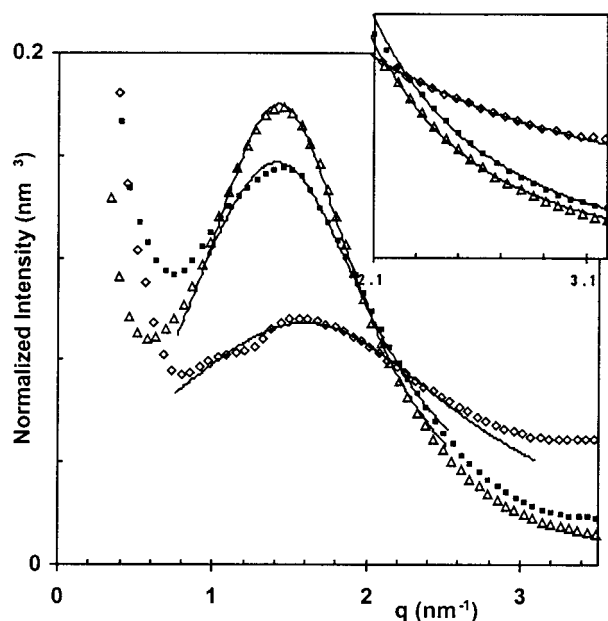


Figure 6. SAXS data for the I725 series collected at room temperature: \diamond , I725-12; \blacksquare , I725-25; \triangle , I725-40. Data have been normalized by the square of the electron density contrast. Only 20% of the data points have been shown. Solid lines are Lorentzian fits to the peaks. The inset shows a magnified view of the data at high q and the power law fits to eq 10.

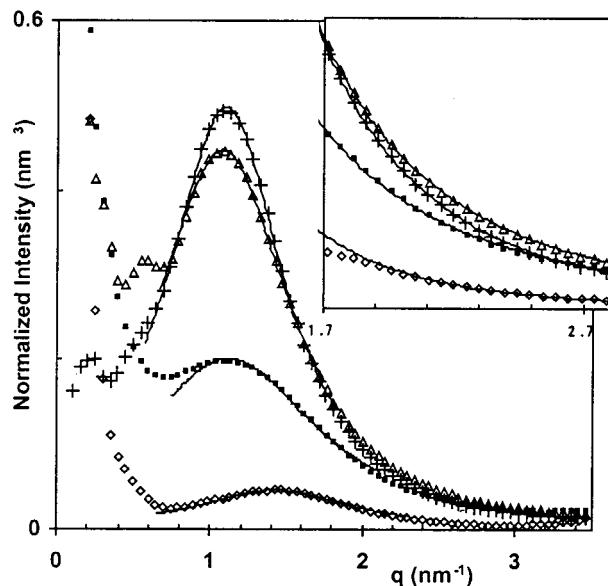


Figure 7. SAXS data for the I1000 series collected at room temperature: \diamond , I1000-0; \blacksquare , I1000-13; \triangle , I1000-32; $+$, I1000-40. Data have been normalized by the square of the electron density contrast. Only 20% of the data points have been shown. Solid lines are Lorentzian fits to the peaks. The inset shows a magnified view of the data at high q and the power law fits to eq 10.

spacing. These will be considered quantitatively in the next section.

One of the goals of this work is to try to correlate changes in viscoelastic properties with those in the microstructure, and hence high-temperature scattering experiments were also performed on these materials. Because of the low viscosity of I725-12, high-temperature experiments were confounded by sample flow; hence, reliable data could not be obtained over a wide temperature range. All other samples (except I2000-0 discussed below) showed no major change in scattering

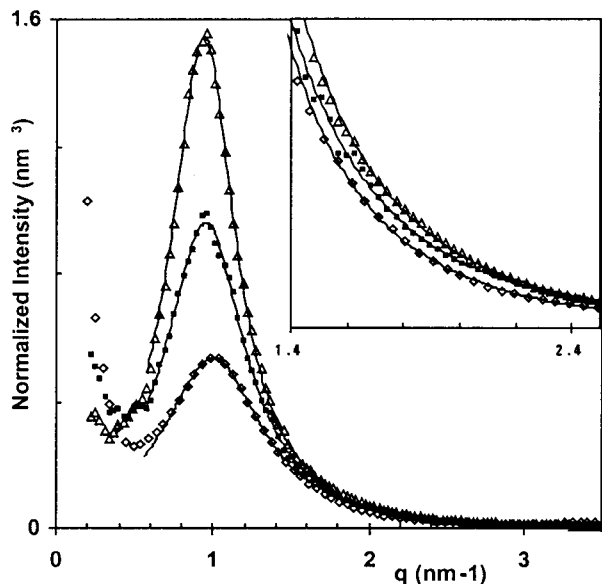


Figure 8. SAXS data for the I2000 series collected at room temperature: \diamond , I2000-0; \blacksquare , I2000-14; \triangle , I2000-20. Data have been normalized by the square of the electron density contrast. Only 20% of the data points have been shown. Solid lines are Lorentzian fits to the peaks. The inset shows a magnified view of the data at high q and the power law fits to eq 10.

with temperature up to 130 °C. Some changes in intensity ($\sim 10\%$) were observed; however, these were neither systematic nor reproducible and probably related to small changes in sample thickness due to flow. Careful analysis of the data by fitting a Lorentzian form (see below) to the peaks showed small shifts toward lower q with increasing temperature in all samples. (I725-12 was not analyzed due poor quality of high-temperature data.) However, these shifts were small ($\sim 0.05\text{--}0.1\text{ nm}^{-1}$ from 30 to 120 °C) compared to the relatively large width of the peaks ($\sim 0.5\text{--}2\text{ nm}^{-1}$), making them difficult to quantify with high accuracy. Therefore, they have not been tabulated in this paper. This decrease in peak position as temperature increases is very unusual^{28,29} and will be commented on in the Discussion section.

Figure 9 shows the effects of temperature on the scattering of I2000-0; it is seen that the intensity decreases considerably between 30 and 120 °C. Like the other samples, there is also a slight shift in the peak position toward lower q as temperature increases. These data are qualitatively similar to the data observed for the sample E3000 published previously⁴ and will be treated more quantitatively in the next section.

3.2.3. Quantitative Analysis of Scattering Data.

This section is composed of two parts: the effects of quaternization (analysis of Figures 6–8) and the effects of temperature on I2000-0 (analysis of Figure 9).

The first quantity of interest is the long spacing for each material. Given that the weight fraction of each block is close to 50%, it is reasonable to assume that all the polyurethanes studied here have a lamellar morphology. The dominant wavelength of this structure, the long spacing d , may be estimated from the position, q_{\max} , of the peak in the Lorentz-corrected scattered intensity $q^2 I(q)$ vs q data as

$$d = \frac{2\pi}{q_{\max}} \quad (12)$$

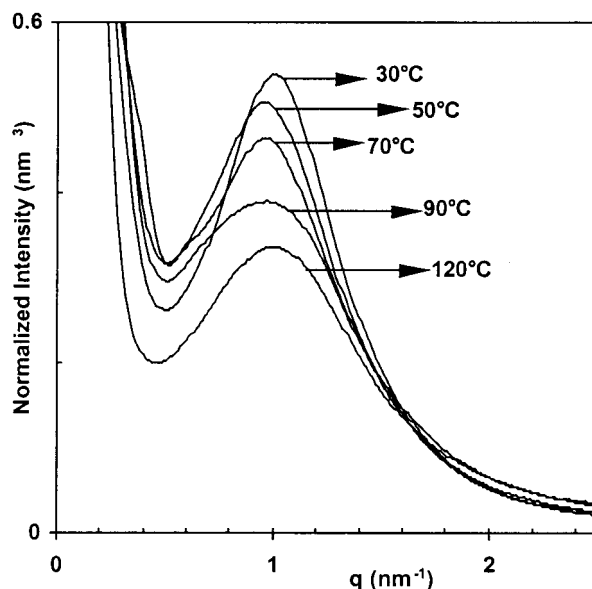


Figure 9. SAXS data for I2000-0 as a function of temperature.

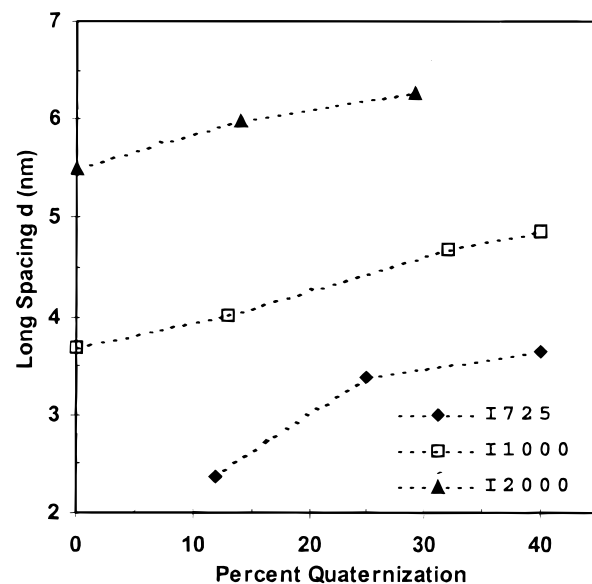


Figure 10. Long spacings in polyurethane cationomers.

Because of the large width of the peaks of some samples and poor statistical quality of others, the $I(q)$ vs q data were first fit to a Lorentzian form

$$L(q) = \frac{k w^2}{w^2 + (q - m)^2} \quad (13)$$

where m is the peak position, $2w$ is the full width at half-maximum, and k is the peak height. The values of m , w , and k are tabulated in Table 3. The peak in $q^2 L(q)$ was taken as the peak of the Lorentz-corrected SAXS pattern; thus, $q_{\max} = m + w^2/m$ which has also been tabulated in Table 3. The corresponding long spacings calculated from eq 12 are shown in Figure 10. As expected, a comparison of the three series shows that long spacing d increases with block length. In addition, d is also seen to increase with quaternization (i.e., incompatibility) within each series especially at low quaternization, indicating that increasing incompatibility causes chain stretching.^{30,31}

The other quantity of interest is the SAXS invariant since as mentioned in section 3.2.1, Q/Q_{\max} is often used

as an estimate of the degree of microphase separation. Calculation of Q as per eq 7 requires extrapolation of the intensity to $q \rightarrow 0$ and $q \rightarrow \infty$; the contribution of the low- q extrapolation to the total invariant is usually small. In our past work,⁴ extrapolation to large q was performed by assuming Porod's law $I(q) = q^{-4}$. The insets of Figures 6–8 and the values of n listed in Table 3 show that Porod's law is clearly not valid for the present materials. One possibility is to arbitrarily assume that the power law form $I(q) = q^{-n}$ of eq 10 is valid to $q \rightarrow \infty$; however, the very low values of n for some samples gives unreasonably high invariants. (Note that the invariant will diverge unless $n > 3$.) Moreover, the calculated invariant showed very strong sensitivity to the background intensity I_b which was often a large fraction of the total intensity due to weak scattering from some samples. Hence, invariants (and the degree of microphase separation) have not been presented here. We instead examine the peak intensities (i.e., values of k in eq 13) presented in Table 3 which are seen to increase with quaternization as well as block length, indicative of increasing microphase separation. Since there is a large change in peak width and position with block length and quaternization, it may be more appropriate to compare the peak intensities in the Lorentz-corrected data $q^2 L(q)$. These values, equal to $k(m^2 + w^2)$, have been shown in the last column of Table 3; these also increase with block length and quaternization. The anomalously large value for I725-12 is probably due to improper background subtraction which heavily influences the data since this sample is a very weak scatterer.

Having considered the effects of quaternization at room temperature, we now turn to a quantitative analysis of the effects of temperature on I2000-0 (Figure 9). This analysis will follow that performed on E3000 published previously, except that unlike the E3000 sample, invariants cannot be calculated reliably as explained in the previous paragraph. Instead, data of Figure 9 were fit to a Lorentzian form (eq 13), $L(q)$ was scaled by q^2 (Lorentz correction), and the corresponding peak intensities $= k(w^2 + m^2)$ were used for the analysis. Data collected at temperatures above 90 °C have not been used due to uncertainty caused by sample flow during data acquisition. As expected from Figure 9, the value of $k(w^2 + m^2)$ was found to decrease upon heating I2000-0 from 30 to 90 °C. It is conventional to plot this change in intensity in the form suggested by mean field theory³²

$$\frac{1}{I(q_{\max})} \sim \text{constant} - 2\chi N_0 \sim k_1 + \frac{k_2}{T} \quad (14)$$

This has been done in Figure 11a. It is found that the data are linear within experimental error in accordance with mean field theory (eq 14), and the extrapolation of the straight line to $(\text{intensity})^{-1} = 0$ (i.e., intensity $\rightarrow \infty$) yields a mean field estimate of 198 K = -75 °C for the spinodal temperature. This application of mean field theory may be checked for self-consistency by testing the approach to the spinodal temperature as³²

$$I(q_{\max}) \sim ((\chi N_0)_s - (\chi N_0))^{-\gamma} \sim \left(1 - \frac{T_s}{T}\right)^{-\gamma} \quad (15)$$

where mean field theory predicts the exponent $\gamma = 1.33$. This is verified in Figure 11b, and the slope of -0.96 is

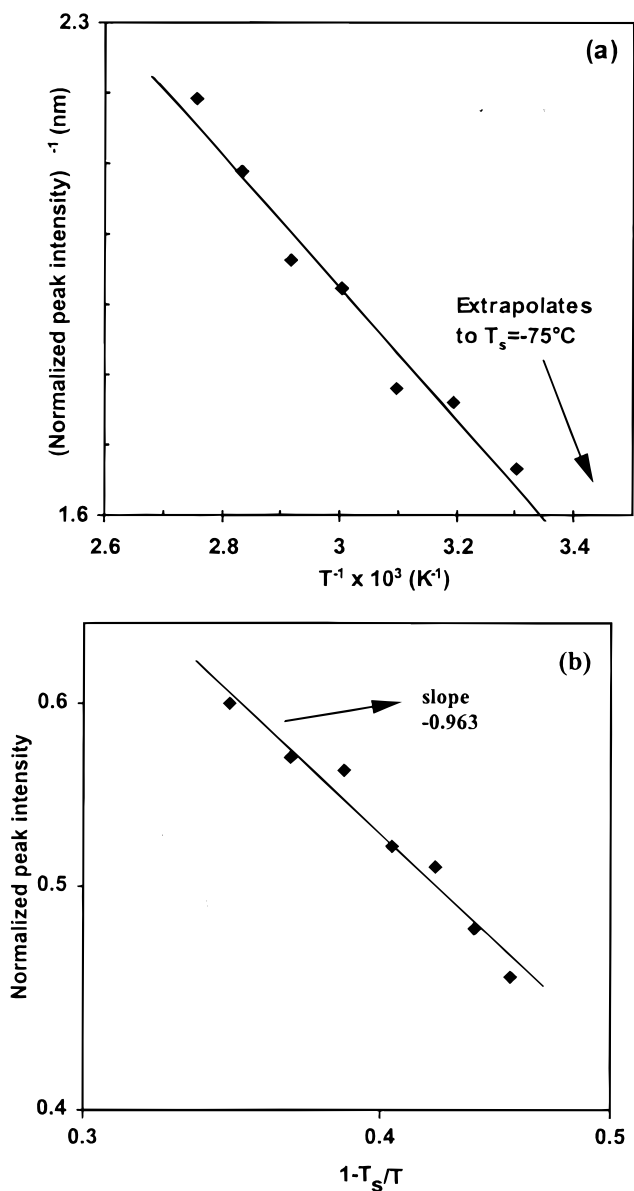


Figure 11. (a) Peak intensities for I2000-0 and the mean field theory estimate of the spinodal temperature. (b) Test of self-consistency for mean field theory; predicted slope = -1 as per eq 15. Note that both axes are logarithmic.

found to be in reasonable agreement with the mean field prediction of -1. It is not possible, of course, to test whether I2000-0 has an ODT close to $T_s = -75$ °C because it is below the soft-segment T_g . In any case, it is unlikely that a polyurethane with as much segmental polydispersity as I2000-0 can undergo a transition into an ordered state. Note that the results of Figure 11 are not seriously dependent on the method of quantifying the peak intensity. Any reasonable means of estimating the peak intensity will allow fitting eq 14 and eq 15 with $\gamma \sim 1$, although a different value of T_s may be obtained.¹¹

4. Discussion

In this section, we attempt to classify materials as single-phase, microphase-separated, or undergoing microphase mixing with increasing temperature. Before attempting this, it is worthwhile understanding two complicating aspects of polyurethanes, both relating to segment length polydispersity which is usually large in polyurethanes. The following discussion is expected to

be generally applicable to block copolymers that are synthesized without precise control of their architecture.

4.1. Segment Length Polydispersity: Effect on Peak Position. The first aspect is directly related to segmental polydispersity. A block copolymer with monodisperse blocks that is far above its ODT is expected to show a correlation hole peak at finite q in its scattering data.³⁴ The intensity of this peak is expected to grow upon approaching the ODT or the spinodal point.³⁵ The position of the peak is expected to be constant far above the ODT³⁵ and then decrease as increasing incompatibility causes chain stretching.³⁰ On the other hand, the position of the peak is expected to be quite different if the blocks are polydisperse. It has been predicted^{36,37} that if block length polydispersity is large, the scattering pattern of a homogeneous block copolymer melt has a peak at $q = 0$ rather than at finite q . As incompatibility is increased, the peak is predicted to stay at $q = 0$ until the spinodal point is crossed; then the peak is predicted to continuously move away from $q = 0$ to progressively larger q as shorter blocks microphase-separate and decrease the wavelength of composition fluctuations.²⁹ Thus, at any temperature, only blocks that are longer than a certain length are microphase-separated. In contrast, block copolymers with monodisperse blocks "do not have the luxury of selecting different portions of the sequence length distribution"²⁹ for microphase separation at different temperatures. This physical picture of selective segregation of the longest blocks has been used by Stein and Koberstein^{38,39} to model microphase separation of polyurethane hard segments. Upon further increasing χ , chain stretching is expected to shift the peak back to lower q ; obviously, this cannot be accounted for within a mean field framework²⁹ which ignores chain stretching. This polydispersity-dependent peak position and the unusual dependence of the peak position on χ can complicate interpretation of SAXS patterns of polyurethanes, especially if the block length polydispersity is not quantitatively known.

This discussion of polydispersity effects lays the ground for pointing out an inconsistency in our data regarding the dependence of long spacing (or the peak position, q_{\max}) on incompatibility. It was mentioned in section 3.2.2 that increasing incompatibility by lowering temperature ($\chi \sim a + bT^{-1}$) causes q_{\max} to increase slightly. This increase in q_{\max} with χ is consistent with the above picture of successively shorter blocks undergoing microphase separation with increasing χ , a behavior that is peculiar to block copolymers with large block length polydispersity. On the other hand, increasing incompatibility by increasing quaternization causes a decrease in q_{\max} (Table 3); this may be interpreted as the effect of chain stretching and is generally expected in all block copolymers at high incompatibility. In the present materials, this change in q_{\max} is very large at low quaternization, indicating that quaternization has a large effect on incompatibility. We have no explanation for this contradictory behavior upon increasing χ by decreasing temperature in one case and increasing quaternization in the other case. One possibility is that increasing quaternization has effects other than simply increasing block incompatibility.

It should be noted that an increase in long spacing with temperature can also result if a poorly developed initial morphology is refined upon heating to higher temperature. The scattering from some samples was remeasured at 30 °C after high-temperature experi-

ments and found to be comparable to the scattering prior to high-temperature experiments. This suggests that there is no significant refinement of morphology upon heating; however, the limited number of such experiments does not conclusively rule out this possibility.

4.2. Segment Length Polydispersity: Effect on Long-Range Order. The second effect of block length polydispersity is on the state of order below the ODT temperature. For block copolymers with monodisperse blocks, the composition fluctuations driving the phase transition can organize into patterns that possess long-range order, giving rise to various morphologies such as bcc spheres, hexagonally packed cylinders, etc. On the other hand, if the blocks are polydisperse, due to the different wavelengths preferred by different blocks, long-range order is unlikely. Accordingly, Fredrickson et al.²⁹ have demonstrated that if blocks are polydisperse, the free energy of a microphase-separated structure is fairly insensitive to long-range order. By minimizing the free energy of such a microphase-separated structure without long-range order, Fredrickson et al.²⁹ have predicted the binodal curve of multiblock copolymers with polydisperse blocks. In accordance with this reasoning, the high polydispersity of polyurethane blocks causes the microphase-separated state of polyurethanes to lack long-range order; this has been noted previously.^{4,28} The primary manifestation of this lack of long-range order is the absence of high-order peaks in SAXS data of polyurethanes. This causes serious experimental difficulties as explained below.

As is well-known from the literature, Liebler's mean field theory³⁵ that predicts an ODT takes no account of composition fluctuations, which have been accounted for in later theories. The effect of composition fluctuations can be fairly large: the experimental ODT temperature may be lower than the mean field estimate by as much as 100 °C, and root-mean-square order parameter fluctuations $\langle \psi(r)^2 \rangle^{1/2}$ may be as much as 0.25 just above the ODT³¹ due to composition fluctuations. (For readers familiar with the polyurethane literature, $\langle \psi(r)^2 \rangle$ is roughly equivalent to the degree of microphase separation Q/Q_{\max} , which is usually between 0.2 and 0.5 for polyurethanes. However, quantitative comparison of $\langle \psi(r)^2 \rangle$ and the degree of microphase separation is not really justified since most of the polyurethane data referred to crystalline blocks.) It is now generally accepted that in many block copolymers, due to composition fluctuations in the disordered state, the local structure is almost the same above and below the ODT;^{31,40} the main role of the ODT is to cause ordering i.e., to impose a large correlation length on the composition fluctuations.

This raises the following question: if there are strong composition fluctuations above the ODT temperature, and the microphase-separated state below the ODT temperature lacks long-range order, how may the ODT be located experimentally? A common criterion for a sample below its ODT, viz. the presence of higher order scattering peaks, is inapplicable since even highly microphase-separated samples will not show higher order peaks if there is no long-range order. Other criteria such as abrupt changes in the width or intensity of the primary scattering peak at the ODT are not likely to succeed since the primary peak is only sensitive to local order which may not change much at the ODT.³¹ (The most reliable method of locating the binodal, viz.

using linear viscoelastic properties, has been discussed in the companion paper.)

Apart from experimental difficulties in locating the ODT, a more fundamental issue is as follows: Is there any justification for making a distinction between a "microphase-separated" state with no long-range order and a nominally "homogeneous" state that has strong composition fluctuations? For a block copolymer in which long-range order is unlikely even with considerable microphase separation, is the idea of an ODT meaningful? Are there any criteria that will allow distinction between the homogeneous and microphase-separated states and thereby define a binodal curve separating them? The next two sections will attempt to answer the last question on theoretical and practical grounds.

4.3. Classification of Materials: Theoretical Considerations. For the present samples, we may attempt a classification between "microphase-separated" and "homogeneous" using the following theoretical predictions:

(1) If segment length polydispersity is very low, the peak position is independent of temperature above the binodal³⁵ (i.e., weak segregation regime) and then moves to lower q as chain stretching occurs. Since polyurethanes are known to have high block length polydispersity, this prediction is probably inapplicable here and will not be discussed below.

(2) If segment length polydispersity is large enough, scattering above the binodal curve has a peak at $q = 0$. If polydispersity is sufficiently small, the peak is at finite q . This is a mean field prediction and ignores effects of strong composition fluctuations.^{29,36,37}

(3) If polydispersity is large, upon increasing incompatibility (i.e., lowering temperature) from the homogeneous state, the peak moves to higher q as successively shorter segments microphase-separate.²⁹ However, as increasing incompatibility causes chain stretching, the peak is expected to move back to lower q .

(4) The intensity at high q may be represented with the dependence of q^{-n} . Above the binodal, $n = 2$ regardless of polydispersity if composition fluctuations are ignored. Composition fluctuations may be expected to increase n . Below the binodal, the dependence must be considerably stronger; $n = 4$ if interfaces are sharp as per Porod's law.

(5) If cooled from above the binodal, the spinodal temperature must be approached in a fashion predicted by eqs 14 and 15. The prediction of $\gamma = 1$ depends on mean field assumptions.³²

(6) Far below the binodal, the intensity must become relatively insensitive to temperature (or incompatibility) since microphase separation is essentially complete. Far above the binodal, the intensity must also become insensitive to temperature, as implied by eq 14 since scattering is purely due to excluded-volume effects. These predictions of course cannot distinguish between above and below the binodal at all; they are mentioned here only because most of the materials studied showed no change in scattering intensity with temperature, and it is important to note that that does not, by itself, provide any conclusions.

The criteria above are fairly ambiguous, indicating that in the absence of higher order peaks distinguishing between "homogeneous" and "microphase-separated" states from SAXS data is a nontrivial task. Moreover, even qualitative aspects of the above predictions depend

on block polydispersity. Hence, in the absence of quantitative knowledge of polydispersity, no progress may be made at all. It is however plausible to assume that the block length polydispersity is fairly high,⁴¹ especially for the hard segments. With this assumption, let us consider the polyurethanes studied here.

Since all polyurethanes have a peak at finite q , criterion 2 based on the mean field theory of Fredrickson et al.²⁹ indicates that they are all below the binodal (provided, of course, that composition fluctuations are small). Criterion 3 based on the same theory predicts that below the spinodal the peak moves to higher q with increasing χ (decreasing temperature). The slight increase in q_{\max} with decreasing temperature mentioned in section 3.2.2 supports this prediction. However, as pointed out in section 3.2.3, increasing χ by increasing quaternization causes a decrease in q_{\max} indicating that there is significant chain stretching. Changes in peak position with quaternization are small at high quaternization; nevertheless, there is certainly no evidence for a decrease in q_{\max} with quaternization. Clearly, the experimental data are ambiguous with respect to (2) and (3) above.

Table 3 presents the values of n for applying criterion 4 which indicates that n generally increases with increasing incompatibility (with the I1000-0 data being anomalous). This prediction is difficult to test due to poor statistical quality of data, limited range of data, and the arbitrariness of choosing the q range for evaluating n . Therefore, the n listed in Table 3, which is an average of at least three independent samples, has fairly large error bars. Nevertheless, as per criterion 4, the I2000 series, I1000-40, and I725-40 may be regarded as highly microphase-separated and I725-12 as almost homogeneous.

Finally, criterion 5 may be applied to I2000-0, which indicates that I2000-0 is well above its spinodal temperature ($T_s = -75$ °C as per Figure 11b), and mean field theory is quantitatively satisfied with $\gamma = 1$. This directly contradicts criterion 4 applied to I2000-0 in the previous paragraph.

Clearly, even assuming that polydispersity is large, the above predictions cannot reach a definitive conclusion about the phase state of most materials presented here. Given the additional uncertainty in the block polydispersity, we abandon the effort of doing this on the basis of theoretical predictions.

4.4. Classification of Materials: Practical Considerations. The primary objective of this research was to study the viscoelastic properties of polyurethane elastomers. Thus, from the point of view of the accompanying paper, the presence or absence of two distinct microphases is important. Hence, although a fundamental classification based on theoretical criteria was unsuccessful in the previous section, classification of the 11 polyurethanes as microphase-separated or microphase-mixed is desirable as a practical matter. The commonly accepted criteria for classifying a polyurethane as microphase-separated are (i) the presence of a low-temperature glass transition (i.e., close to that of the pure soft segment), (ii) the presence of a low-temperature peak in the E' (or $\tan \delta$) in a dynamic mechanical temperature sweep experiment and the presence of a plateau in E' above this peak temperature, and (iii) the presence of a "strong" peak in the SAXS data.

Of these, the DSC and the dynamic mechanical analysis are usually more important since these are directly related to the elastomeric properties of the polyurethane. The last one is somewhat arbitrary since scattering intensity depends severely on the electron density contrast between the segments. On the basis of these "practical" criteria, the following classification is made.

I725-0 and I1000-0 are almost completely microphase-mixed as per all three of the above criteria. (Dynamic mechanical data will be presented in the accompanying paper.) In I1000-32, I1000-40, and all I2000 materials, the presence of two microphases is not in doubt since these satisfy the first two criteria listed above. These materials will be regarded as being considerably microphase-separated. The remaining materials are microphase-separated to varying extents. Finally, as per the scattering data of Figure 9, I2000-0 will be regarded as gradually microphase-mixing as temperature increases. In this case, the microphase compositions may be regarded as changing continuously with temperature, rather than exhibiting an abrupt microphase-mixing transition at a specific temperature.

5. Summary

In this second part of our ongoing research on the viscoelastic properties of polyurethane elastomers, we have reported on the synthesis and structural characterization of a series of polyurethane cationomers with pendant trialkylammonium groups. Three series differing in block length were synthesized, and the materials within each series had fixed composition, block length, and molecular weight. By changing the extent of quaternization of the pendant dimethylammonium groups, the segmental incompatibility may be varied greatly, and these materials ranged from almost completely homogeneous to highly microphase-separated.

From the DSC data, it was found that the I725 series was almost homogeneous, whereas the I2000 series was almost completely microphase separated. Annealing at high temperatures followed by quenching at high rates caused no visible change in the DSC traces, making it impossible to construct microphase composition vs temperature phase diagrams for these polyurethanes.

The SAXS patterns of most materials underwent no significant change with increasing temperature, except for a slight decrease in the peak position q_{\max} . The direction of this shift in q_{\max} is opposite of that expected in monodisperse block copolymers and is consistent with the interpretation that, in block copolymers with polydisperse blocks, increasing incompatibility causes successively shorter blocks to microphase-separate and increase q_{\max} . However, the increasing incompatibility with quaternization contradicted this expectation by causing q_{\max} to reduce significantly.

I2000-0 was seen to undergo gradual microphase mixing as temperature increases from 30 to 120 °C. The changes in peak intensity were consistent with a mean-field-like approach to the spinodal temperature from above it. The spinodal temperature was found to be -75 °C although other data indicate that I2000-0 is highly microphase separated even at room temperature.

The scattering results of this paper demonstrate the ambiguity of distinguishing between the "homogeneous" and the "microphase-separated" states when the former has strong composition fluctuations and the latter has no long-range order. There seems to be no justification for making such a distinction from a practical viewpoint.

An ODT is not meaningful for materials that lack long-range order, and it seems rather difficult to experimentally define a binodal curve separating the "homogeneous" and the "microphase-separated" states. This view will be reinforced by the results of linear viscoelastic experiments in the accompanying paper.

Acknowledgment. We are grateful to Dr. Roger Phillips, Montell Inc., USA, for valuable comments about this manuscript and especially for suggesting that the power-law behavior of the high- q data is relevant to section 4.3. We thank Ms. Leata Damouth for her assistance with some of the DSC experiments. This work was funded by the Army Research Office.

References and Notes

- (1) Hepburn, C. *Polyurethane Elastomers*, 2nd ed.; Elsevier Applied Science Publ.: London, 1991.
- (2) Wirpsza, Z. *Polyurethanes: Chemistry, Technology and Application*; Harwood Pubs.: New York, 1993.
- (3) Lamba, N. M. K.; Woodhouse, K. A.; Cooper, S. L. *Polyurethanes in Biomedical Applications*; CRC Press: Boca Raton, FL, 1998.
- (4) Velankar, S.; Cooper, S. L. *Macromolecules* **1998**, *31*, 9181.
- (5) Ferry, J. D. *Viscoelastic Properties of Polymers*; John Wiley and Sons: New York, 1980.
- (6) Flory, P. J. *Principles of Polymer Chemistry*; Cornell University Press: Ithaca, NY, 1953.
- (7) Chen, T. K.; Chui, J. Y.; Shieh, T. S. *Macromolecules* **1997**, *30*, 5068.
- (8) Goddard, R. J.; Cooper, S. L. *J. Polym. Sci., Polym. Phys. Ed.* **1994**, *32*, 1557.
- (9) Goddard, R. J.; Cooper, S. L. *Macromolecules* **1995**, *28*, 1390.
- (10) Goddard, R. J.; Cooper, S. L. *Macromolecules* **1995**, *28*, 1401.
- (11) Velankar, S. Ph.D., University of Delaware, 1999.
- (12) Miller, J. A.; Cooper, S. L. *J. Polym. Sci., Polym. Phys.* **1985**, *23*, 1065.
- (13) Velankar, S.; Cooper, S. L. *Macromolecules* **2000**, *33*, 395.
- (14) Speckhard, T. A.; Hwang, K. K. S.; Cooper, S. L.; Chang, V. S. C.; Kennedy, J. P. *Polymer* **1985**, *26*, 70.
- (15) Leung, L. M.; Koberstein, J. T. *Macromolecules* **1986**, *19*, 706.
- (16) Koberstein, J. T.; Galambos, A. F. *Macromolecules* **1992**, *25*, 5618.
- (17) Phillips, R. A.; Stevenson, J. C.; Nagarajan, M. R.; Cooper, S. L. *J. Macromol. Sci. Phys.* **1988**, *B27*, 245.
- (18) Couchman, P. R. *Macromolecules* **1978**, *11*, 1156.
- (19) Glatter, O.; Kratky, O. *Small Angle X-Ray Scattering*; Academic Press: London, 1982.
- (20) Balta-Calleja, F. J.; Vonk, C. G. *X-Ray Scattering of Synthetic Polymers*; Elsevier Science Publishers: Amsterdam, 1989; Vol. 8.
- (21) van Bogart, J. W. C.; Gibson, P. E.; Cooper, S. L. *J. Polym. Sci., Polym. Phys. Ed.* **1983**, *21*, 65.
- (22) Speckhard, T. A.; Gibson, P. E.; Cooper, S. L.; Chang, V. S. C.; Kennedy, J. P. *Polymer* **1985**, *26*, 55.
- (23) Koberstein, J. T.; Stein, R. S. *J. Polym. Sci., Polym. Phys. Ed.* **1983**, *21*, 2181.
- (24) Tyagi, D.; McGrath, J. E.; Wilkes, G. L. *Polym. Eng. Sci.* **1986**, *26*, 1371.
- (25) Vonk, C. G. *J. Appl. Crystallogr.* **1973**, *6*, 81.
- (26) Ruland, W. *J. Appl. Crystallogr.* **1971**, *4*, 70.
- (27) Koberstein, J. T.; Morra, B.; Stein, R. S. *J. Appl. Crystallogr.* **1980**, *13*, 34.
- (28) Ryan, A. J.; Macosko, C. W.; Bras, W. *Macromolecules* **1992**, *25*, 6277.
- (29) Fredrickson, G. H.; Milner, S. T.; Leibler, L. *Macromolecules* **1992**, *25*, 6341.
- (30) Almdal, K.; Rosedale, J. H.; Bates, F. S.; Wignall, G. D.; Fredrickson, G. H. *Phys. Rev. Lett.* **1990**, *65*, 1112.
- (31) Rosedale, J. H.; Bates, F. S.; Almdal, K.; Mortensen, K.; Wignall, G. D. *Macromolecules* **1995**, *28*, 1429.
- (32) Bates, F. S.; Hartney, M. A. *Macromolecules* **1985**, *18*, 4278.
- (33) Stanley, H. E. *Introduction to Phase Transitions and Critical Phenomena*; Oxford University Press: Oxford, 1971.
- (34) de Gennes, P. G. *Scaling Concepts in Polymer Physics*; Cornell University Press: Ithaca, NY, 1979.
- (35) Leibler, L. *Macromolecules* **1980**, *13*, 1602.
- (36) Benoit, H.; Hadziioannou, G. *Macromolecules* **1988**, *21*, 1449.

- (37) de Gennes, P. G. *Faraday Discuss. Chem. Soc.* **1979**, 68, 96.
- (38) Koberstein, J. T.; Stein, R. S. *J. Polym. Sci., Polym. Phys. Ed.* **1983**, 21, 1439.
- (39) Koberstein, J. T.; Galambos, A. F.; Leung, L. M. *Macromolecules* **1992**, 25, 6195.
- (40) Dalvi, M. C.; Eastman, C. E.; Lodge, T. P. *Phys. Rev. Lett.* **1993**, 71, 2591.
- (41) Peebles, L. H. *Macromolecules* **1974**, 7, 872.

MA990817G